

## Field and temperature dependence of the $c$ -axis critical current in $\text{Bi}_2\text{Sr}_2\text{CaCu}_2\text{O}_{8+\delta}$ single crystals at the melting and two-dimensional decomposition fields

Sheng Luo,\* Guang Yang,<sup>†</sup> and C. E. Gough\*

*Superconducting Research Group, University of Birmingham, Birmingham B15 2TT, United Kingdom*

(Received 28 July 1994)

Measurements of the  $V$ - $I$  characteristics and critical currents along the  $c$  axis are reported for a number of small single crystals of  $\text{Bi}_2\text{Sr}_2\text{CaCu}_2\text{O}_{8+\delta}$  as a function of temperature, magnetic field, and oxygen stoichiometry. The primary aim of this investigation was to investigate changes in the  $c$ -axis resistivity resulting from misalignment of pancake vortices across superconducting  $\text{CuO}_2$  planes at the melting and 3D-2D decomposition fields. Although the field dependence of the critical current is shown to scale with the field at which the 3D-2D decomposition takes place, no significant change in the field dependence was observed at either phase transition. This implies a short-range correlation of the positions of pancake vortices across planes persisting well above such transitions.

### I. INTRODUCTION

$\text{Bi}_2\text{Sr}_2\text{CaCu}_2\text{O}_{8+\delta}$  (2212-BSCCO) is an extremely anisotropic high- $T_c$  superconductor with anisotropy factor  $\gamma = (m_c/m_{ab})^{1/2} = \lambda_c/\lambda_{ab}$  that can be as large as 300–1000.<sup>1–3</sup> Lawrence-Doniach<sup>4</sup> (LD) proposed an appropriate microscopic model for such superconductors, in which superconductivity in the weakly superconducting  $c$  direction involves Josephson tunneling between superconducting planes. A single crystal of BSCCO can therefore be considered as a series array of large-area SIS junctions, with 0.3-nm-thick superconducting  $\text{CuO}_2$  double-layer electrodes separated by 1.2-nm-thick  $\text{Bi}_2\text{Sr}_2\text{O}_4$  insulating layers. Kleiner *et al.*<sup>5</sup> have reported Josephson tunneling characteristics along the  $c$  axis of BSCCO single crystals in addition to both direct and indirect ac Josephson effects, providing strong support for such a model.

In the LD model, flux threads through the crystal in the form of quantized flux pancakes with current largely confined to the  $\text{CuO}_2$  planes.<sup>6,7</sup> At low temperatures and magnetic fields, such pancakes in the absence of pinning will align to form a quasi-three-dimensional (3D) flux-line lattice essentially identical to the Abrikosov flux-lattice structure expected for extremely anisotropic 3D superconductors.

Recent  $\mu\text{SR}$  (Ref. 8) and neutron-diffraction<sup>9</sup> measurements have confirmed the existence of such a lattice, but only for low fields ( $< 0.1$  T) and temperatures below the irreversibility line. In these measurements the flux lattice was observed to undergo a melting transition<sup>10</sup> at the irreversibility line independently determined from magnetic measurements on the same samples.<sup>9</sup> Below the irreversibility line, on increasing field, another transition was observed to a state with a much reduced correlation in flux pancake alignment along the  $c$  direction, identified as the field  $B_{2D}$  at which the 3D flux-line lattice decomposes into a 2D layered structure,<sup>11</sup> with little correlation in position of flux pancakes between adjacent superconducting bilayers.

Such a transition is predicted at a field  $B_{2D} \sim \phi_0/(\gamma d)^2$ ,<sup>9,10</sup> where  $d$  is the spacing between superconducting bilayers, when the interplane coupling of pancake vortices become smaller than their coupling within the planes. Measurements of magnetic hysteresis on the same samples used for neutron diffraction and  $\mu\text{SR}$  studies show that this transition occurs at the same field as the onset of the “arrowhead anomaly” in irreversible magnetization measurements.<sup>9</sup> The sudden increase in magnetic hysteresis above the 3D-2D phase transition was initially tentatively identified with increased pinning of vortex pancakes above the 3D-2D transition by extended planar dislocation networks.<sup>12</sup> This has recently been confirmed by magnetic decoration and TEM measurements on the same 2212-BSCCO crystal specimens by Grigorieva *et al.*<sup>13</sup>

Any loss of alignment of flux pancakes across planes resulting from either melting or 3D-2D decomposition transitions would be expected to lead to a significant reduction in the critical current along the  $c$  direction.<sup>14</sup> The influence of thermal fluctuations and of randomly dispersed pinning centers on the alignment of pancake vortices and the resulting  $c$ -axis critical current has been theoretically modeled by Daemen *et al.*<sup>15</sup> Thermal fluctuations of the positions of the pancake vortices are predicted to result in a strongly temperature-dependent field dependence of the  $c$ -axis critical current. For moderate anisotropy parameter  $\gamma$ , a first-order 3D-2D decoupling transition has been predicted, which becomes second order for large anisotropies.

The above authors also considered the perturbation in position of a 3D lattice of flux pancakes by randomly distributed pinning centers on each plane. This results in a field-dependent reduction in  $c$ -axis critical current  $j_c = j_0 \exp(-B/B^*)$ , where  $B^*$  depends on the density of pinning centers, which is shown to be consistent with our measurements at low fields. The effect of pinning on the 3D-2D decomposition transition was not considered, though it was anticipated to occur at high fields, whereas in practice the transition occurs at relatively modest

fields  $\sim 30\text{--}100$  mT.<sup>9,10</sup> In this paper, we present measurements of the  $c$ -axis  $V$ - $I$  characteristics in the normal and superconducting states for a number of 2212-BSCCO single crystals subjected to different processing conditions to vary the oxygen stoichiometry in the insulating planes and hence the anisotropy factor  $\gamma$ .<sup>16</sup> Measurements have been made over a range of fields and temperatures to compare with the theoretical models above.

Below  $T_c$ , we have concentrated on measurements of the critical current over the range of fields that melting and 3D-2D transitions have been inferred from neutron-diffraction<sup>9</sup> and  $\mu$ SR (Ref. 8) measurements. The critical current in all crystals investigated decreases monotonically with increasing field at all temperatures, with no evidence for any discontinuity in value or any significant change in field dependence either on crossing the irreversibility line at the melting transition or on crossing the decomposition transition on increasing field. This implies a persistent correlation in position of flux pancakes across adjacent pairs of  $\text{CuO}_2$  planes extending well above these transitions. The effective correlation length along the  $c$  axis must therefore be somewhat greater than the spacing between the superconducting double  $\text{CuO}_2$  layers ( $d > 1$  nm). An upper limit for the correlation length can be deduced from  $\mu$ SR measurements,  $\sim \lambda_{ab} \sim 200$  nm. This is significantly smaller than the upper limit deduced from neutron-diffraction measurements ( $\sim 10$   $\mu\text{m}$ ).<sup>17</sup>

We also present measurements of the  $c$ -axis  $V$ - $I$  characteristics above  $T_c$ , similar to measurements reported elsewhere (see Kleiner *et al.*<sup>5</sup> for extensive references to earlier measurements). In contrast to the resistivity in the  $ab$  plane, the resistance in the  $c$  direction, at small currents, *increases* on approaching  $T_c$  from above. However, the  $V$ - $I$  characteristics, at least for oxygen-doped crystals, are very nonlinear in this region and the increased resistivity may be in part be associated with thermal fluctuations of the superconducting order parameter, which decreases the density of states of normal electrons above  $T_c$  and also their lifetimes.<sup>18–21</sup>

Surprisingly few authors have commented on the nonlinear  $V$ - $I$  characteristics above  $T_c$  and most only quote resistances measured at low currents. At larger currents,

the resistance at all temperatures appears to approach a limiting “normal-state” value. This limiting resistance decreases slowly with decreasing temperature, even well below  $T_c$ , as evident from the  $V$ - $I$  characteristics well above  $T_c$ . When modeling measurements below  $T_c$ , we assume it is this high-current resistance value that provides the damping of the series of resistively shunted junctions (RSJ). This then results in realistic estimates for the effective interlayer capacitance, deduced from the current at which  $V$ - $I$  characteristics start to become hysteretic.

## II. EXPERIMENT

Measurements of the electrical characteristics along the  $c$  direction have been made on a number of small single crystals using a method that is essentially identical to the described by Kleiner *et al.*<sup>3</sup> The crystals were grown using a large temperature gradient growth technique.<sup>22</sup> Samples were cleaved and shaped from larger crystals of similar quality to those used for neutron-diffraction,<sup>9</sup>  $\mu$ SR,<sup>8</sup> and magnetic measurements.<sup>13</sup> The influence of oxygen stoichiometry, and hence anisotropy factor  $\gamma$ , on our measurements was investigated using as-grown (AG) crystals, vacuum annealed (VA) crystals, and oxygen annealed (OA) crystals, as described in Table I.

Typical sample sizes ranged from  $30 \times 30 \times 5$   $\mu\text{m}$  to  $100 \times 150 \times 10$   $\mu\text{m}$ . The small size of the crystals was determined by the requirement that their lateral dimensions should be less than  $\lambda_c$  ( $> 100$   $\mu\text{m}$  for our samples, see Table I). We can then assume short-junction behavior between layers, with no vortices parallel to the layers induced by self-currents.

Because of the extreme difficulty of attaching leads to such small crystals, only two-point measurements of the  $V$ - $I$  characteristics were possible. To minimize the contact resistance, a gold layer was sputtered on to the opposite faces of the crystals and also on to the 0.3-mm-diam flattened cone faces of the spring-loaded metal rods used to make electrical contact. From the residual slope of the resistance in the superconducting state at low temperatures, any normal component of the contact resistance

TABLE I. BSCCO(2212) single-crystal characterization.

Sample number	Annealing condition	Sample dimension ( $\mu\text{m}^3$ )	$\lambda_c$ ( $\mu\text{m}$ ) (4.2 K)	$T_c$ (K) ( $\Delta T$ )	$j_c$ (4.2 K) ( $\text{A}/\text{cm}^2$ )	$\rho$ ( $T_c$ ) ( $\Omega \text{cm}$ )	$\beta$ (4.2 K)	$C$ ( $\text{F}/\text{m}^2$ )	$\Delta^*$ (4.2 K) (meV)	$\Delta^*/\Delta_{\text{BCS}}$ (%)
B10	$2 \times 10^{-5}$ mbar 420°C 25 h	$150 \times 110 \times 10$	493	87(5)	70	100	3.1	0.035	0.38	3
B5	As grown	$120 \times 100 \times 12$		93.0(10)		10				
B13	As grown	$40 \times 50 \times 4$		90.6(9)	370	6.5				
B15	As grown	$30 \times 30 \times 8$	162	93.0(9)	670	7.2	11	0.27	0.38	3
B6	500°C O2 72 h	$110 \times 90 \times 10$		86(2.5)		4.95				
B11	500°C O2 72 h	$30 \times 50 \times 6$		85.7(2.7)	1240	5.25				
B12	500°C O2 72 h	$30 \times 40 \times 5$	117	87.5(4)	1275	5.0	11.8	0.105	0.28	2

was estimated to be always less than  $\sim 5\%$  of the total sample resistance. No corrections have been made for the contact resistances in data presented in this paper.

Measurements were made in a continuous-flow cryostat with the sample directly cooled by flowing helium. An external field of up to 0.25 T could be applied at any angle between the *c* axis and *ab* plane.

### III. MEASUREMENTS

Typical *V-I* characteristics for an oxygen-annealed crystal (*B12*) as a function of temperature in zero and 0.1 T field are shown in Figs. 1(a) and 1(b). These curves illustrate the main features of the characteristics on cooling. In particular, we note (i) the nonlinearity at small currents, which becomes significant well above  $T_c$  ( $\sim 87$  K for this sample); (ii) the development of a superconducting transition below  $T_c$ , with *V-I* characteristics becoming increasingly hysteretic on decreasing temperature; and (iii) the influence of magnetic field on such features. Superimposed *V-I* measurements at a few representative temperatures are replotted in Fig. 2, which allow a more direct comparison of the magnitudes of the current-induced superconducting transitions. At large currents, it will be noted that the resistance approaches a temperature-independent "normal-state" value.

The *c*-axis resistivity measured at small currents is illustrated in Figs. 3(a)–3(c) for vacuum-annealed (VA), as-grown (AG), and oxygen-annealed (OA) crystals. These measurements show the strong dependence of normal-state resistivity on sample oxygenation, with a value that increases dramatically close to  $T_c$ . This is most pronounced for the vacuum-annealed crystal, which is the most anisotropic.

The increased *c*-axis resistivity of BSSCO on cooling has been associated with thermally activated hopping between conducting  $\text{CuO}_2$  planes<sup>23</sup> and with an intrinsic dependence associated with spin-charge separation by Anderson.<sup>24</sup> Recently, Balestrino *et al.*<sup>20</sup> have fitted the enhanced *c*-axis resistivity in thin 2212-BSCCO films to a fluctuation model introduced by Ioffe *et al.*,<sup>19</sup> who derive a quasi-logarithmic *c*-axis resistance varying as  $R = R_n / F(T)$ , where

$$F(T) = \int_0^\infty \frac{dx}{8x \cosh^2(x/4)} \text{Im}[\sqrt{\kappa + (\lambda + ix)^2}] \\ \times \left[ \frac{x^2 + \lambda^2}{|\kappa + (\lambda + ix)^2|} + 1 \right]$$

with  $\kappa = \kappa_0 \ln[T_c / (T - T_c)]$ , where  $\kappa_0 = 18.7 T_c / \varepsilon_F$  in the clean limit and  $\kappa_0 = 2 / (\tau_\phi^2 \varepsilon_F T_c)$  for strong dephasing of superconducting quasiparticles with dephasing time  $\tau_\phi$ ;  $\lambda$  is of order unity for moderate in-plane scattering and is small for low in-plane scattering. Such a model with  $\lambda$  small and  $\kappa_0 \sim 1$  (the values inferred by Balestrino *et al.*<sup>20</sup> from measurements on 2212-BSCCO thin films) would account qualitatively for the upturn in resistivity for our as-grown and oxygen-annealed crystals over a restricted range of temperatures near  $T_c$ . However, the changes in resistivity for the vacuum-annealed crystal occur over too

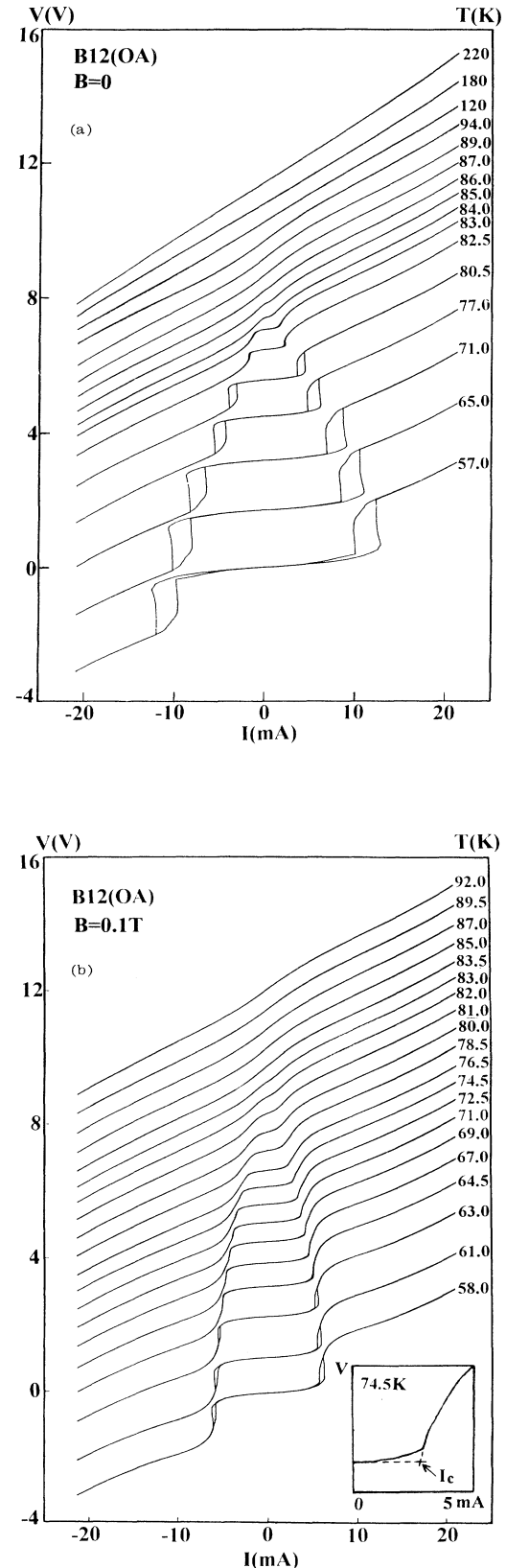


FIG. 1. The temperature dependence of the *c*-axis *V-I* characteristics for sample *B12* (OA) and (a) zero field and (b) 0.1 T. The inset illustrates how the critical current  $I_c$  was defined.

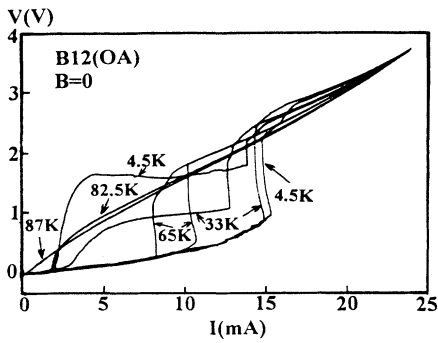


FIG. 2. Superimposed  $c$ -axis  $V$ - $I$  curves for sample  $B12$  (OA) at 4.5, 33, 65, 82.5, and 87 K.

wide a range of temperatures to be described by any such model, which requires that  $(T - T_c)/T_c$  is small. Further detailed investigation of the nonlinear  $V$ - $I$  characteristics above  $T_c$  are required, and especially of the influence of doping, as this may shed light on the nature of electron transport in the  $c$  direction.

On cooling below  $T_c$ , the  $V$ - $I$  characteristics are initial-

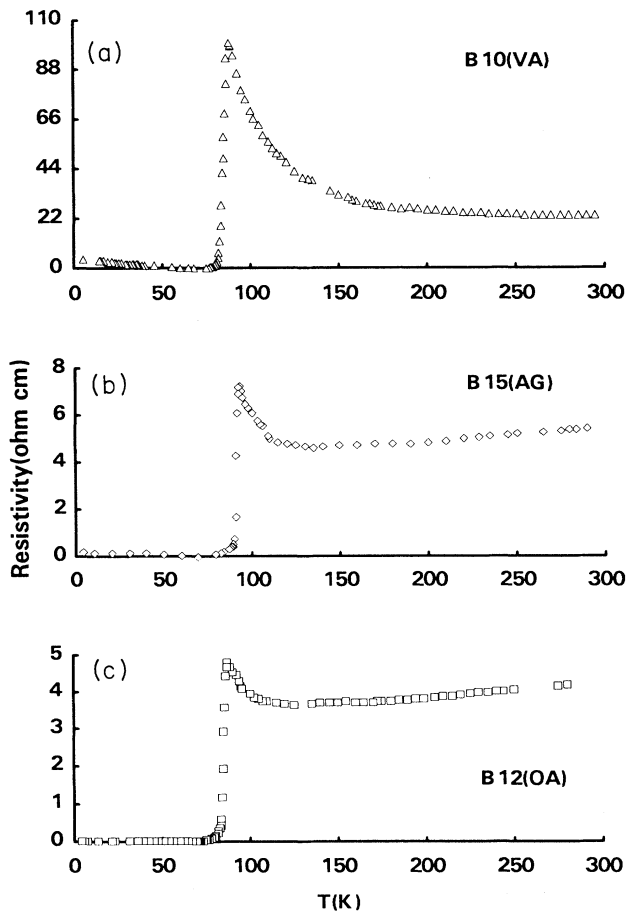


FIG. 3. The  $c$ -axis small current resistivity for (a) sample  $B10$  (vacuum annealed), (b) sample  $B15$  (as grown), and (c) sample  $B12$  (oxygen annealed).

ly reversible with a thermally broadened superconducting transition. We define a value for  $I_c$  in this regime as the current at zero voltage extrapolated from the region of steepest slope of the  $V$ - $I$  characteristics, as illustrated by the inset in Fig. 1(b). At lower temperatures, the transition occurs at a clearly defined critical current  $I_c$ . As the sample is further cooled, the  $V$ - $I$  characteristics become increasingly hysteretic. This is consistent with the behavior expected from the RSJ model for the individual junctions, when the McCumber parameter,<sup>25</sup>  $\beta_c$ , exceeds unity. It will be noted that the measured  $V$ - $I$  characteristics are slightly reentrant above  $I_c$ . This arises because the current was provided by a voltage source with a series resistance. Above the superconducting transition, a significant amount of power is dissipated inside the crystal (typically  $>10$  mW in the fully developed normal state), which results in a decrease in critical current and the observed reentrant characteristics. We have no way of correcting for any temperature change that arises from such heating, though the crystal is directly cooled by flowing helium gas.

An approximate estimate of the temperature rise at the center of the crystal from self-heating can be made by assuming uniform power dissipation and heat flow along the  $c$  axis only. Unfortunately, there are no published measurements of the  $c$ -axis thermal conductivity down to low temperatures. However, measurements at around 50 K and above by Crommie *et al.*<sup>23</sup> would suggest a low-temperature conductivity varying approximately as  $0.01 T \text{ WK}^{-1} \text{ m}^{-1}$ , though measurements of thermal conductivity in the  $ab$  plane are typically ten times higher.<sup>26</sup> For a  $100\text{-}\mu\text{m}$  square,  $5\text{-}\mu\text{m}$ -thick crystal the Crommie *et al.* value would result in a temperature rise of  $\sim 12.5/T$  K, per mW power dissipated in the bulk of the crystal, showing that heating is likely to be a very serious problem in the normal state for currents exceeding  $I_c$ . Fortunately heating is not likely to be such a problem at the initial transition from the superconducting state, which is used to define  $I_c$ . As the temperature rise is proportional to the square of the thickness of the crystal, it is important to use as thin crystals as possible for such measurements. In practice we were limited by the difficulties in handling and making contacts to crystals smaller than those used.

At high temperatures, the characteristics are consistent with almost all the bilayer junctions (typically  $\sim 3000$ ) undergoing a simultaneous transition to the normal state over a relatively narrow range of currents. However, at low temperatures, small differences in critical currents across individual layers lead to early transitions. On increasing current, discrete superconducting transitions are then observed from different regions of the thickness, as is evident in the 4.5- and 33-K measurements in Fig. 2. For such measurements we identify the intrinsic bulk  $I_c$  as the current at which the major change in voltage is observed, which typically involves  $>70\%$  of the junctions undergoing a simultaneous transition, as judged by the relative change in resistivity at the transition. Differences in superconducting properties across the sample are not unexpected because of the likely presence of microcracks, dislocation networks, variations in oxygen

stoichiometry, modification of surface properties close to the contact regions and other crystal defects.

The critical current density of our crystals increases systematically with oxygenation, as shown in Table I. The temperature dependence of the normalized critical current is plotted for a number of representative crystals in Fig. 4. The critical currents for the as-grown and oxygen-annealed samples approach a limiting low-temperature value consistent with SIS rather than SNS behavior. For these samples, the critical currents tend to lie slightly above the Ambegaokar-Baratoff predictions<sup>27</sup> for the temperature dependence of an ideal SIS junction,  $I_c(T)R_n = (\pi\Delta/2e)\tanh(\Delta/2kT)$ , indicated by the solid line in Fig. 4, and there is a small upturn of the critical current at the lowest temperatures, which might be an indication of a small self-heating effect. Self-heating is almost certainly significant for the vacuum-annealed sample, where the effective sample temperature is almost certainly above that of the surrounding helium, resulting in an experimental curve with a resistance continuing to rise down to the lowest temperatures.

The values of the effective energy gap  $\Delta^*$  (values listed in Table I) derived from the measured voltage change at  $I_c$  for all our crystals were typically only a few percent of the value expected from the BCS relation  $2\Delta_{\text{BCS}} = 3.75kT_c$ . In contrast, Kleiner *et al.*,<sup>3</sup> observed voltage steps  $\sim 15$  mV, close to the expected BCS value. These measurements were deduced from early transitions as the critical current was exceeded in individual layers. However, such values were only observed in their argon-grown single crystals: in oxygen-annealed and Pb-doped crystals, much smaller values of  $\Delta^*$  were deduced from the major transition at  $I_c$ , though they still tended to be slightly larger than derived for our crystals. Similar low values for  $\Delta^*$  have also been deduced in measurements by Kadowaki *et al.*<sup>28</sup> It is well known that defects in artificial SIS junctions can reduce measured  $I_cR$  products well below theoretical values. Furthermore, in practice the bulk critical current will always be limited by the weakest junctions with the smallest critical currents, which will be particularly important if heating in such

junctions result in an avalanche process.

The  $V$ - $I$  characteristics are predicted to become hysteretic, when the McCumber parameter  $\beta_c = 2\pi C I_c R^2 / \Phi_0 = 1$ , where  $R$  is the interplanar resistance (total resistance/number of junctions in thickness of crystal) and  $C$  is the interplanar capacitance. Assuming that  $R$  is determined by the resistance measured at larger rather than small currents, we can use the onset of hysteresis to estimate the capacitance and hence effective dielectric constant between superconducting layers. From zero-field measurements, we obtain capacitances in the range  $0.035$ – $0.27$  Fm<sup>-2</sup>, corresponding to an effective dielectric constant varying from 30 in the vacuum-annealed sample to 3 in the oxygen-annealed sample. These values should be compared with the value of dielectric constant  $\sim 25$  suggested by recent measurements of the low-frequency transverse plasma resonance<sup>29</sup> in BSCCO single crystals.<sup>30</sup> Anything other than order-of-magnitude agreement would be fortuitous, as we cannot assume ideal SIS behavior for the individual junctions. We have ignored thermal broadening of the transition and the influence of superconducting fluctuations, which would further complicate any detailed interpretation of our measurements.

The exact form of the hysteretic characteristics of a series array of RSJ junctions will depend on the effective electromagnetic coupling between layers and the outside world. Although no attempt has yet been made to describe the exact form of the characteristics on decreasing current, it is important to note the increase in voltage observed in the measurements at low temperatures (see Fig. 2). Such behavior is not expected for a simple RSJ junction model, for which the voltage would be expected to decrease monotonically before switching back to the superconducting state. We observe similar features to those shown in Fig. 2 for all our samples at low temperatures but the features is most pronounced in the oxygen-annealed samples. An explanation in terms of self-heating would seem to be ruled out, as the effective resistance for the 4.5 K measurements rises well above the "normal-state" value. Similar characteristics have recently been observed in measurements on small mesas lithographically patterned on the surface of single crystals of BSCCO,<sup>31</sup> where the authors interpret their measurements in terms of nonequilibrium self-injection of quasiparticles, which reduces superconductivity, as inferred from measurements on artificial arrays of conventional superconductor junctions.<sup>32,33</sup> It seems likely that similar effects are also present in bulk HTC crystals.

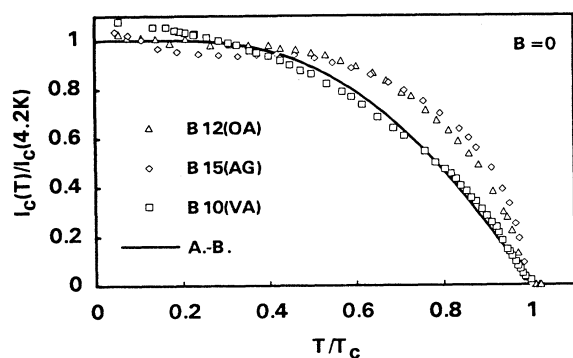


FIG. 4. The temperature dependence of the normalized *c*-axis critical current for samples B10 (VA), B15 (AG), and B12 (OA). The solid line is the Ambegaokar-Baratoff relation for SIS junctions.

#### IV. INFLUENCE OF MAGNETIC FIELD

Comparison of Figs. 1(a) and 1(b) show that, on applying a field in the *c* direction, the critical current is depressed and the transition is slightly broadened, with the onset of hysteretic behavior raised to a somewhat larger value of  $I_c$ . This is a further demonstration that the actual dynamics is more complicated than predicted by a simple McCumber model, since  $\beta_c$  should only depend on  $I_c$ .

Figure 5 shows the dependence on field of the normalized critical current for an oxygen-annealed sample at a

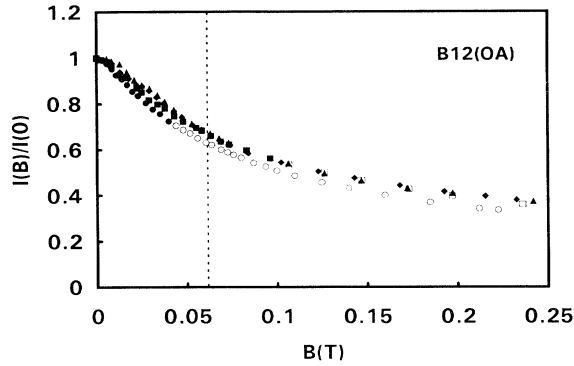


FIG. 5. The field dependence of the normalized  $c$ -axis critical current for sample  $B12$  (OA) at  $T=4.2$  K (solid triangles), 25 K (solid diamonds), 50 K (squares), and 60 K (circles). The magnetically determined 3D-2D transition field for this sample is indicated by the dashed vertical line. Solid and open symbols represent measurements taken below and above the magnetically determined irreversibility line, respectively.

number of temperatures. The field dependence of the critical current is only weakly dependent on temperature for all our crystals, irrespective of oxygenation. In particular, there is no evidence for any significant change in  $I_c$  or its field dependence at either the 3D-2D decomposition transition field or the irreversibility line marking the melting transition. In Fig. 5 the approximately temperature-independent 3D-2D transition field  $B_{2D}$  is indicated by the dashed vertical line and measurements below and above the magnetically determined irreversibility line are indicated by open and solid symbols, respectively.

These results immediately imply a relatively strong correlation in the positions of flux pancakes across the planes, persisting to fields and temperatures well above the 3D-2D decomposition and irreversibility line transitions. Although the reported measurements were made as a function of increasing magnetic field, our measurements were ideally reversible to within our experimental accuracy. The reversibility is a consequence of the small size and relatively weak pinning of our crystals.

Figure 6 shows the field dependence of the critical current at 25 K normalized to its zero-field value for three crystals; vacuum annealed, as grown, and oxygen annealed. The field dependence is strongly dependent on the state of sample oxygenation.

All three curves can be plotted on a single universal curve, illustrated in Fig. 7, using as the scaling field  $B_{2D}$ , the field at which the 3D-2D decomposition transition is known to occur as deduced from  $\mu$ SR and neutron-diffraction measurements on similarly processed crystals. These values were confirmed by direct magnetic measurements on the parent crystals from which the resistivity samples were cleaved, identifying the 3D-2D transition as the onset field of the magnetic arrowhead anomaly. The universal curve can be fitted over a wide field range by an empirical relationship of the form  $\alpha \exp(-B/B_1^*)$

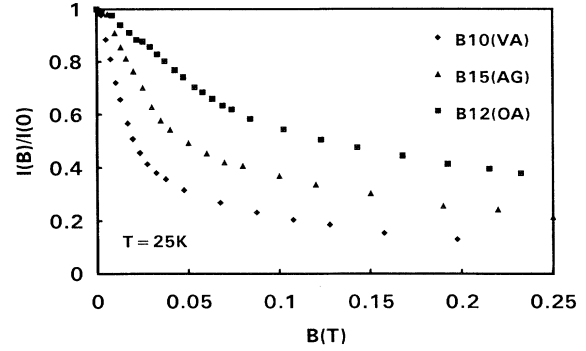


FIG. 6. The field dependence of the normalized  $c$ -axis critical current at 25 K for crystals  $B10$  (VA),  $B15$  (AG), and  $B12$  (OA).

$+\beta \exp(-B/B_2^*)$ , where  $\alpha=0.71$ ,  $\beta=0.34$ ,  $B_1^*=1.67B_{2D}$ , and  $B_2^*=20.5B_{2D}$ .

In a small number of cases, we also measured the critical current as a function of field direction relative to the  $c$  axis. Except for field directions very close to the  $ab$  planes, the critical current was determined by the component of field along the  $c$  axis, as previously demonstrated by Kleiner *et al.*<sup>3</sup>

The suppression of the critical current density by misalignment of flux lines across opposing electrodes of a Josephson junction was first considered by Miller *et al.*<sup>14</sup> These ideas were extended by Daemen *et al.* (DBMC),<sup>15</sup> who considered two situations: thermally activated decomposition of a 3D lattice of pancake vortices and pinning-induced disorder of the 3D lattice.

All the above models assume that the Josephson current is determined by the difference in phase across adjacent pairs of superconducting  $\text{CuO}_2$  planes. If pancake vortices are well ordered across the planes, the spatial variation of the phase on one plane exactly matches the spatial variations of phase on the neighboring planes.

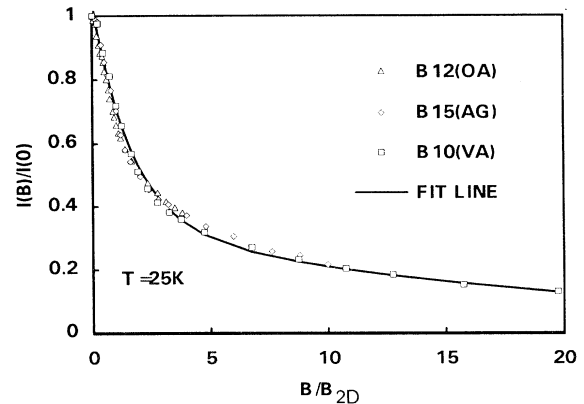


FIG. 7.  $I(B)/I(0)$  vs  $B/B_{2D}$  curves for samples  $B10$  (VA),  $B15$  (AG), and  $B12$  (OA). The curves can be fitted by a universal empirical relationship of the form  $I(B)/I(0) = 0.71 \exp(-0.60B/B_{2D}) + 0.34 \exp(-0.05B/B_{2D})$ . The scaling field  $B_{2D}$  was derived from independent magnetic measurements with values 10, 25, and 62 mT, respectively.

Therefore, to first order the presence of pancake vortices should not affect the critical current along the  $c$  axis. However, if the positions of individual pancakes are perturbed by thermal fluctuations or are shifted by interactions with nearby defects, phase coherence across adjacent planes is lost resulting in a reduction of the  $c$ -axis critical current.

DBMC showed that thermal fluctuations should lead to a 3D-2D phase transition of pancake vortices at a field  $B_{2D}$  that was predicted to vary strongly with temperature. Furthermore, fluctuations were predicted to give rise to a reduction in  $c$ -axis critical current with a field dependence varying strongly with temperature. In contrast,  $\mu$ SR and neutron-diffraction measurements show that the decomposition field is relatively insensitive to temperature, and the depression of critical current with field is remarkably insensitive to temperature (Fig. 4). DBMC also predict the existence of a totally uncorrelated pancake vortex structure above the 3D-2D decomposition field, with a vanishingly small  $c$ -axis critical current, whereas we always observe a finite critical current extending to fields well above those at which the transition is expected from  $\mu$ SR and neutron-diffraction measurements. Thermal fluctuations therefore appear not to be important at the temperatures and fields investigated in these measurements.

Daemen *et al.*<sup>15</sup> also considered the influence of random pinning on a 3D pancake lattice as flux lines cross each  $\text{CuO}_2$  bilayer. The resulting misalignment of pancakes across planes gives rise to an approximately exponential decrease in  $c$ -axis critical current with increasing field,  $j_c = j_0 \exp(-B/B^*)$ , where  $B^* = 8\Phi_0/\pi n^2 u_0^6$  and  $B^* = 2n\Phi_0/\pi$  for small and large pinning densities, respectively;  $n$  is the aerial density of pinning centers within individual  $\text{CuO}_2$  bilayers, and  $u_0 \sim \lambda_J = \gamma s$  is the Josephson length, where  $s$  is the periodicity of the superconducting planes.

Such a model can be compared with our measurements at low temperatures and fields, where the pancakes are ordered in a 3D lattice. The spacing of the flux lines below the 3D-2D decomposition is  $> 1 \mu\text{m}$ , which is significantly larger than the expected spacing of defects in the  $\text{CuO}_2$  planes (oxygen vacancies and extended dislocation networks).<sup>34</sup> It is therefore reasonable to assume that we are in a strong pinning density regime, with each pancake pinned to a nearby pinning center within the  $\text{CuO}_2$  planes. We indeed observe a nearly linear reduction in critical current with field at low fields (see Fig. 6), which would imply a density of pinning centers,  $n \sim \pi B^*/2\Phi_0$ , where  $B^* \sim 3B_{2D}$ . This gives characteristic length scales for the distance between pinning centers in the  $\text{CuO}_2$  planes of  $\sim 200$ ,  $\sim 140$ , and  $\sim 80$  nm for the vacuum-annealed, as-grown, and oxygen-annealed crystals, respectively.

The above model implies an increase in the number of pinning centers on increased oxygenation, whereas the number of individual oxygen vacancy pinning sites will obviously decrease. However, it is known that the density of planar dislocation networks increases on oxygenation.<sup>12</sup> Such defects have been confirmed as strong pinning sites in 2212-BSCCO.<sup>13</sup> The characteristic pinning

length associated with such networks is  $\sim 200$  nm, which is similar to the pinning length scales derived above.

From Fig. 7, we note that the field dependence cannot be described by a single exponential curve over the whole field range. The deviation from the predicted field dependence could reflect a change in coherence of pancakes across planes at the 3D-2D decomposition transition.

A detailed description of the field dependence of the  $c$ -axis critical current will almost certainly have to take into account the influence of random pinning centers in addition to the intrinsic coupling between layers governed by the anisotropy factor  $\gamma$ . A self-consistent model must also be able to account for the melting and 3D-2D transitions in terms of both anisotropy factor and random pinning.

Whatever the origin of the pinning, the above measurements demonstrate a very strong correlation between the field dependence of the  $c$ -axis critical current with associated scaling field  $B^*$  and  $B_{2D}$ , the field at which the 3D-2D decomposition takes place. This correlation may simply be accidental, but on face value it suggests that the density of pinning centers in the  $\text{CuO}_2$  planes may be just as important as the anisotropy factor  $\gamma$  in determining the field at which the 3D-2D transition takes place.

## V. SUMMARY

Measurements of the electrical characteristics of BSCCO single crystals along the  $c$  axis are shown to be consistent with a model for such crystals as a series array of RSJ junctions. Although such a model accounts qualitatively for the observed  $V$ - $I$  characteristics and provides a sensible estimate for the effective interplane capacitance, the values of critical current observed are significantly smaller than those expected from the Ambegaokar-Baratoff relation.

The  $V$ - $I$  characteristics above  $T_c$  are highly nonlinear, at least for the oxygen-annealed crystal, possibly consistent with a fluctuation enhanced resistance at low currents (or voltages) associated with the excitation of virtual Cooper pairs. However, the fractional change in resistance of the vacuum-annealed crystal between room temperature and  $T_c$  is probably too large to be described by superconducting fluctuations alone.

No strong evidence is found for any marked change in value or field dependence of the critical current at either the 3D-2D lattice decomposition field or the melting transition at the irreversibility line. This implies that flux pancakes remain relatively well correlated in position across planes well above these transitions, even though the spatial correlation disappears on the length scales probed by neutron-diffraction and  $\mu$ SR measurements.

The field dependence of the critical current at small fields is consistent with the existence of a 3D flux lattice of vortex pancakes that is perturbed by local pinning on crossing each  $\text{CuO}_2$  plane. A simple model for such pinning leads to the observed quasiexponential decrease in critical current, but the observed dependence is slower at larger fields, implying a stronger than predicted persistent correlation of pancakes between planes. Hence the fields  $B_{2D}$  and  $B_{irr}$  at which the 3D-2D and melting

transitions are inferred from neutron-diffraction,  $\mu$ SR, and magnetization measurements involve phase transitions occurring over length scales greater than the spacing between the  $\text{CuO}_2$  double layers.

The field dependence of the normalized critical current can be described by a universal function using as the scaling field, the field  $B_{2D}$  at which the 3D-2D transition is inferred from neutron-diffraction,  $\mu$ SR, and magnetic measurements. This field is strongly influenced by the state of oxygenation of the sample, and hence by the anisotropy factor  $\gamma$ . However, the situation is further complicated because increased oxygenation also increases the number of planar dislocation networks, which provide effective pinning centers, thus complicating any theoretical interpretation of experimental data. Further model-

ing studies are required to clarify the influence of in-plane defects on the 3D-2D decomposition and melting transitions and to consider the influence of such transitions on the  $c$ -axis critical current.

#### ACKNOWLEDGMENTS

We gratefully acknowledge helpful discussions with Ted Forgan, Bob Cubbit, Bea Avenhaus, Yusheng He, and L. N. Bulaevsky. This research is supported by the Engineering and Physical Sciences Research Council, UK. One of us (S.L.) is grateful for the award of an Overseas Research Studentship.

- \*School of Physics and Space Research, University of Birmingham, Birmingham, UK.
- <sup>†</sup>School of Metallurgy and Materials, University of Birmingham, Birmingham, UK.
- <sup>1</sup>D. E. Farrel, S. Bonham, J. Foster, Y. C. Chang, P. Z. Jiang, K. G. Vandervoort, D. L. Lam, and V. G. Kogan, *Phys. Rev. Lett.* **63**, 782 (1989).
- <sup>2</sup>K. Okuda, S. Kawamata, S. Noguchi, N. Itoh, and K. Kadowaki, *J. Phys. Soc. Jpn.* **60**, 3226 (1991).
- <sup>3</sup>R. Kleiner and P. Müller, *Phys. Rev. B* **49**, 1327 (1994).
- <sup>4</sup>W. E. Lawrence and S. Doniach, in *Proceedings of the 12th International Conference on Low Temperature Physics*, edited by E. Kanda (Academic Press of Japan, Kyoto, 1971), p. 361.
- <sup>5</sup>R. Kleiner, F. Steinmeyer, G. Kunkel, and B. Müller, *Phys. Rev. Lett.* **68**, 2394 (1992).
- <sup>6</sup>L. N. Bulaevskii, S. V. Meshkov, and D. Feinberg, *Phys. Rev. B* **43**, 3728 (1991).
- <sup>7</sup>J. R. Clem, *Phys. Rev. B* **43**, 7837 (1991).
- <sup>8</sup>S. L. Lee, P. Zimmermann, H. Keller, M. Warden, I. M. Savic, R. Schauwecker, D. Zech, R. Cubitt, E. M. Forgan, P. H. Kes, T. W. Li, A. A. Menovsky, and Z. Tarnawsky, *Phys. Rev. Lett.* **71**, 3862 (1993).
- <sup>9</sup>R. Cubitt, E. M. Forgan, G. Yang, S. L. Lee, D. McK. Paul, H. A. Mook, M. Yethiraj, P. H. Kes, T. W. Li, A. A. Menovsky, Z. Tarnawski, and K. Mortensen, *Nature* **365**, 407 (1993).
- <sup>10</sup>A. Houghton, R. A. Pelcovits, and S. Subdo, *Phys. Rev. B* **40**, 6763 (1989).
- <sup>11</sup>V. M. Vinokur, P. H. Kes, and A. E. Koshalev, *Phys. Rev. B* **43**, 29 (1990).
- <sup>12</sup>G. Yang, P. Shang, S. D. Sutton, C. E. Gough, and J. S. Abell, *Phys. Rev. B* **48**, 4054 (1993).
- <sup>13</sup>I. V. Grigorieva *et al.*, *Proceedings of the M2S-HTC IV Conference* [Physics C (to be published)].
- <sup>14</sup>S. L. Miller, K. R. Biagi, J. R. Clem, and D. K. Finnemore, *Phys. Rev. B* **31**, 2684 (1985).
- <sup>15</sup>L. L. Daemen, L. N. Bulaevskii, M. P. Maley, and J. Y. Coulter, *Phys. Rev. Lett.* **70**, 1167 (1993); *Phys. Rev. B* **47**, 11291 (1993).
- <sup>16</sup>B. O. Wells, Z. X. Shen, D. S. Dessau, W. E. Spicer, C. G. Olson, D. B. Mitzi, A. Kapitulnik, R. S. List, and A. Arko, *Phys. Rev. Lett.* **65**, 3056 (1990).
- <sup>17</sup>E. M. Forgan (private communication).
- <sup>18</sup>K. E. Gray and D. H. Kim, *Phys. Rev. Lett.* **70**, 1693 (1993).
- <sup>19</sup>L. B. Ioffe, A. I. Larkin, A. A. Varlamov, and L. Yu, *Phys. Rev. B* **47**, 8936 (1993).
- <sup>20</sup>G. Balestrino, M. Marinelli, E. Milani, A. A. Varlamov, and L. Yu, *Phys. Rev. B* **47**, 6037 (1993).
- <sup>21</sup>V. V. Dorin, R. A. Klemm, A. A. Varlamov, A. I. Buzdin, and C. V. Livanov, *Phys. Rev. B* **48**, 12951 (1993).
- <sup>22</sup>G. Yang, C. E. Gough, and J. S. Abell, *IEEE Trans. Appl. Supercond.* **3**, 1663 (1993).
- <sup>23</sup>M. F. Crommie and A. Zettl, *Phys. Rev. B* **43**, 408 (1991).
- <sup>24</sup>P. W. Anderson, *Science* **235**, 1196 (1987); *Phys. Rev. Lett.* **65**, 2306 (1990); **66**, 3226 (1991).
- <sup>25</sup>D. E. McCumber, *J. Appl. Phys.* **39**, 297 (1967).
- <sup>26</sup>N. V. Zavaritsky, A. V. Samoilo, and A. A. Yurgens, *Physica C* **169**, 174 (1990).
- <sup>27</sup>V. Ambegaokar and A. Baratoff, *Phys. Rev. Lett.* **10**, 486 (1963).
- <sup>28</sup>K. Kadowaki, T. Mochiku, H. Takeya, K. Hirata, and Y. Saito, *Proceedings of the M2S-HTC IV Conference* (Ref. 13).
- <sup>29</sup>S. Tajima, G. D. Gu, S. Miyamoto, A. Odagawa, and N. Koshizuka, *Phys. Rev. B* **48**, 16164 (1993).
- <sup>30</sup>M. Tachiki (private communication).
- <sup>31</sup>A. Yurgens, D. Winkler, Y. M. Zhang, N. Zavaritsky, and T. Claeson, *Proceedings of the M2S-HTC IV Conference* (Ref. 13).
- <sup>32</sup>I. Iguchi, *Phys. Rev. B* **16**, 1954 (1977).
- <sup>33</sup>D. Winkler and T. Claeson, *Phys. Scr.* **32**, 317 (1985).
- <sup>34</sup>P. Shang, G. Yang, I. P. Jones, C. E. Gough, and J. S. Abell, *Appl. Phys. Lett.* **63**, 827 (1993).